# Study of Trends in System Efficiency for a Biomass Integrated Gasification Fuel Cell Gas Turbine System when Carbon Dioxide Content is Enhanced

Das Sadiq, Kabir; Aravind, P. V.; Woudstra, T.; Jaiganesh, N.; Ajith kumar, R.

**DOI**
10.1016/j.matpr.2023.04.195

**Publication date**
2023

**Document Version**
Final published version

**Published in**
Materials Today: Proceedings

**Citation (APA)**
Das Sadiq, K., Aravind, P. V., Woudstra, T., Jaiganesh, N., & Ajith kumar, R. (2023). Study of Trends in System Efficiency for a Biomass Integrated Gasification Fuel Cell Gas Turbine System when Carbon Dioxide Content is Enhanced. *Materials Today: Proceedings*, *80*(1), A1-A7. https://doi.org/10.1016/j.matpr.2023.04.195

Materials Today: Proceedings 80 (2023) A1–A7

Contents lists available at ScienceDirect

Materials Today: Proceedings

journal homepage: www.elsevier.com/locate/matpr

# Study of Trends in System Efficiency for a Biomass Integrated Gasification Fuel Cell Gas Turbine System when Carbon Dioxide Content is Enhanced

Kabir Das Sadiq [a], P.V. Aravind [b,c], T. Woudstra [c], N. Jaiganesh [a], R. Ajith kumar [a,*]

[a] Department of Mechanical Engineering, Amrita Vishwa Vidyapeetham, Amritapuri, India
[b] Process and Energy Department, Faculty of 3mE, Delft University of Technology, Leeghwaterstraat 39, 2628, CB, Delft, the Netherlands
[c] Energy and Sustainability Research Institute Groningen, Faculty of Science and Engineering, University of Groningen, the Netherlands

ARTICLE INFO

*Article history:*
Available online 25 April 2023

*Keywords:*
Biomass gasifier
Solid Oxide Fuel Cell
$CO_2$ Gasification
System Efficiency

ABSTRACT

The performance of a 30-kW gasifier–SOFC–GT system was evaluated using thermodynamic calculations. Nickel/Gadolinia Doped Ceria (Ni/GDC) anodes were utilized for Solid Oxide Fuel Cells (SOFCs). These systems can achieve high electrical efficiencies of above 50%. The goal of the study is to evaluate trends in system efficiency when carbon dioxide as a gasifier agent is increased in enhanced carbon dioxide system. Carbon dioxide content was increased in both systems, leading to variants of both systems as compositions changed until they could no longer function efficiently. The trends in system variants were monitored. Although the gross efficiency increased, the net efficiency of the enhanced carbon dioxide system dropped. Absorbed heat and delivered gross which deals with flow of energy in sources / sinks was lower in enhanced scheme. Auxiliary power consumed was higher in enhanced carbon dioxide system variants, indicating that the compressors consume more power. Delivered net power was dropping for the enhanced case variants. Enhanced carbon dioxide system variants seem to have a slightly higher total electrical efficiency by a close range of less than 1%.

Selection and peer-review under responsibility of the scientific committee of the 3rd International Congress on Mechanical and Systems Engineering.

## 1. Introduction

Solid oxide fuel cells (SOFCs) are powered using hydrogen, carbon monoxide, methane, or a combination of these fuels to generate electricity and heat. They can be employed alongside gas turbines that can generate power at high pressures resulting in electricity production. Clean and sustainable power generation using biosyngas as a fuel derived from biomass gasifier has piqued the scientific community's interest for quite some time. [1–9]. As solid fuels, like as biomass, may be gasified to form syngas, they are thought to be suitable for SOFC fueling. Due to their adaptability to a variety of fuels and high efficiency, solid oxide fuel cells (SOFCs) are getting prominence among various fuel cell types. SOFC power systems use the heat generated by the exothermic electrochemical oxidation within the fuel cell for the endothermic steam reforming process to boost efficiency. Its capability to directly accept fuel mixtures of methane, hydrogen, carbon monoxide, carbon dioxide and steam makes it a feasible alternative because it is not poisoned by carbon monoxide and carbon dioxide. Gas cleaning is essential as it utilizes hydrogen, carbon monoxide, and methane in biosyngas to fuel SOFCs. More studies and development in high percentage utilization of biomass in larger-scale power plants is crucial in view of increased environmental concerns and higher emission limits. This is where biomass co-gasification for clean and sustainable electricity generation comes into play [10–13]. Some initiatory studies have mentioned high electric power efficiencies of over 50% for biomass gasifier–SOFC–GT systems [9].

Despite the fact that systems used for gas cleaning at lower temperatures are more efficient and likely yield better results, extensive gas cleansing is still essential. It is often implied that higher temperature gas cleaning systems, which are currently being developed, will result in improved efficiency and better heat transfer capabilities. Various cleaning techniques that function at various temperatures are frequently recommended in the publica-

* Corresponding author.
*E-mail address:* amritanjali.ajith@gmail.com (R. Ajith kumar).

https://doi.org/10.1016/j.matpr.2023.04.195
2214-7853/
Selection and peer-review under responsibility of the scientific committee of the 3rd International Congress on Mechanical and Systems Engineering.

tions [1] such as particulates, tar, alkali compounds, and acid gases. This paper examines trends in system efficiency in a biomass integrated gasification fuel cell gas turbine system with increased carbon dioxide content. Here two schemes namely, a base case system and an enhanced carbon dioxide system with preheating air will be considered.

Both schemes will undergo increased carbon dioxide content and the subsequent results of the schemes will be portrayed in this paper briefly outlines their intended operational parameters.

### 1.1. Subsystem utilized

Envisioned systems are designed in cycle tempo software include a biomass gasifier, gas cleaning system, SOFC system, and gas turbine are presented in Figs. 1 & 2.

As depicted the biomass fed into the biomass gasifier producing biosyngas. The biosyngas obtained from gasifier is cleansed and brought into fuel cell, which burns the unspent fuel with unspent outlet stream air from cathode end. The turbine is fueled with flue gas and the subsequent exhaust from the turbine is utilized for preheating the inlet air at cathode and air for gasification.

### 1.2. Gasifier subsystem

The transformation of biomass into gaseous fuel by heating using air, oxygen, or steam as a medium is known as gasification. Gasification, unlike burning, generates biosyngas and a combustible gas from biomass that contains chemical energy when the oxidation process is nearly finished. Exact gas compositions are affected by a variety of factors depending on the consideration of biomass utilized, mode of gasification and gasification agent considered. Cold gas efficiency of around 80 % is expected to be attained as the chemical energy carried in the gas during the conversion of biomass into chemical energy. In the present study air gasification is considered. This is because the gas generated will have relatively low tar when fixed bed co-current gasification is used. The methane generation is less compared to steam gasification when air gasification is employed [1,5]. Compositions of biosyngas nearing equilibrium are produced by fixed bed downdraft type air gasification systems. Cycle tempo is used to verify the gasification process models of such gasifiers. The approach taken by cycle tempo model for the calculations of system efficiency does not have a significant dependence on the presence of methane in the syngas generated. There is no comparison of data and estimated composition values for higher pressures because no measurement data is available. In the base case system as well as enhanced carbon system we have taken a series of readings for air entering the gasifier inlet. We have increased the carbon dioxide content for a series of readings by adjusting carbon dioxide to fuel ratio. Nitrogen and oxygen too have undergone change in composition relatively to subsequent relative increase in carbon dioxide content.

### 1.3. Fuel cell subsystem

Solid Oxide Fuel Cells have been under development for several decades. Due to better contaminant tolerance for biogas-based systems we will be considering anodes of Nickel/Gadolinia Doped Ceria (Ni/GDC) for our SOFC [1,3]. As it becomes obvious, they will almost probably play a significant role in energy systems in the future due to their increased efficiency, much effort is being poured into their development at present. In addition to syngas, they are capable of accepting other hydrocarbon fuels as well. Operating temperatures ranges from 873 to 1273 K. It functions on carbon-based fuels such as $CH_4$, CO etc. [1]. Fuel gas is propagated by the anode of the fuel cell with electrolyte in its interphase. Electrochemical processes are catalyzed by electrons liberated from fuel molecules. The flow of electrons through an external circuit generates electricity. Cathode end spreads oxygen with solid electrolyte in its interphase and transports electrons from the external circuit decreasing the molecules of oxygen, generating oxide ions. The fuel is oxidized in SOFC after it makes its way to the anode chamber. The cathode chamber receives the entering oxygen, where it is ionized and delivered to the anode via the electrolyte. Depending on the kind of fuel, oxide ions flow through the solid electrolyte to the anode to generate $H_2O$ or $CO_2$. Even though the solid electrolyte has several oxygen vacancies, oxygen ions can diffuse. Solid electrolyte primarily inhibits electronic contact between the two electrodes by preventing electrons while retaining overall electrical charge balance by enabling oxide ion flow from the cathode to the anode. This plays a significant role in determining temperature range. Ni/GDC anodes and Lanthanum Strontium Manganite (LSM) cathodes were considered here for SOFC. Since SOFC are still in developmental stage, the stack performance of biosyngas composition is not yet fully explored. The cell performance using various biosyngas can be looked up on [1,5]. Reasonable assumptions based on acceptable values of SOFC model input parameters are shown in Table 2.

### 1.4. The gas turbine - heat recovery subsystem

The gas turbine of power rating of 30 kW was used for the systems. The mass flows throughout the system. The power level is determined by the turbine power rating which is fixed at 30 kW. The system is not thought to reflect any of the commercially available gas turbines. However, we believe that the appropriate properties highlighted in this study can be designed into turbines. The turbine and compressor isentropic and mechanical efficiency figures are based on publications for a capstone turbine of comparable capacity. Exit gases at anode and cathode are partially recirculated in the current system model, as indicated in Fig. 1. Remaining gases at anode and cathode end are routed to the afterburner, and the mixture that is combusted is routed to the inlet of the gas turbine. Output gas from the turbine is utilized to preheat the cathode air, gasify the air, and generate the additional steam required.

### 1.5. SOFC - gas turbine integration

Amount of cooling air essential to maintain appropriate functioning temperature of fuel cell is determined by the fuel. The ability at anode chamber to incorporate endothermic reforming activities aids in increasing fuel cell efficiency. Endothermic reformation occurs when methane is present in the fuel. Cathodic Air flows when reduced can possibly reduce the compression work and heating needed for the air supply at cathode, resulting in the modelling of gasifier is modelled as discussed above in gasifier subsystem. increased SOFC–GT system efficiencies. Efficiency rates of 70–80 percent have been reported for SOFC–GT systems with natural gas as fuel.

### 1.6. Component models and system efficiencies

Cycle-Tempo is a proprietary that was developed in-house. designed at TU Delft's division of energy technology [2,16], is used to do thermodynamic calculations. In the various subsystem models utilized in these computations, Cycle-Tempo utilizes Gibbs free energy minimization-based procedure for equilibrium calculations. The Cycle-Tempo manual has more information on these models. The flow of mass along the turbine, as a result, throughout the system, is determined by the level of turbine's power and other relevant characteristics. The cathode airflow is determined by the

energy balance at the fuel cell, which is based on the cooling air required. Together, these two subsystems have a critical role in estimating the biomass flow into the inlet. As a result, the fundamental equations that drive the mechanisms of fuel cell and gas turbine, are utilized in the Cycle-Tempo computations [16]. This can be used to better understand fluctuations in system performance. The model brings in the incoming gas to equilibrium in the instance of the fuel cell. The active cell area, cell voltage V, current flow I, and electrical output power Pe are all determined after that. The operations are thought to take place at a constant temperature and pressure. The total current is related to the fuel cell and flow through the same, φm,a,in which is shown in the equation.

$$I = \frac{\varphi_{m,a,in}}{M_a} 2F \left( y^0_{H_2} + y^0_{CO} + 4y^0_{CH_4} \right) U_F \tag{1}$$

The inlet concentrations are denoted by yi$^0$, $M_a$ being anode gas mole mass, F stands for faraday constant and $U_F$ is fuel utilization. Using current flow and the energy balance as a guide, the mass flow from the cathode to the anode of oxygen is determined. Since the temperature at the output is known, energy balance dictates cathode airflow. A one-dimensional model of the active surface is employed to determine current density $i_m$, voltage V, and electrical power $P_e$. The flow density distribution in the fuel flow direction is computed in the cell area model. The following local variables. Reversible voltage Ex, Current density $i_x$, Concentrations $y_x$ ($H_2$, CO, $H_2O$, $CO_2$ and $CH_4$).

We could use either of $V_{rev,\ x}$ or $E_{rev,x}$ to obtain Nernst voltage. Expecting gases to behave ideally in a SOFC, the reversible voltage can be expressed as equation below.

$$V_{rev} = V^0_{rev} + \frac{RT}{2F} \ln\{ \frac{y^{\frac{1}{2}}_{O_2,c} y_{H_2,a}}{y_{H_2O,a}} \times P^{\frac{1}{2}}_{cell} \} \tag{2}$$

For hydrogen the standard reversible voltage is$V^0_{rev}$.Universal gas constant denoted by R. Temperature T, Pressure P and at the cross-section, mole fraction is denoted by *y*. The assumption made in the model is that at the level of electrodes, voltage losses are negligible in x direction. As an outcome, across the fuel cell, voltage is considered to be constant.

$$\Delta V_x = V_{rev,x} - V \tag{3}$$

Voltage loss is $\Delta V_x$. In the cross section, current density is given by

$$i_x = \frac{\Delta V_x}{R_{eq}} \tag{4}$$

Equivalent cell resistance denoted by $R_{eq}$. The equation that connects these quantities over the cell is given by

$$\frac{I}{A} = \frac{U_F}{R_{eq} \int_0^{U_F} d\lambda / (V_{rev} - V)} \tag{5}$$

*I* denotes total current, cell area by A, dimensionless reaction coordinate by λ. Power can be calculated when values of current and voltage are known. In the case of a turbine, for an expanded gas the outlet enthalpy can be calculated by

$$h_0 = h_i - \eta_s (h_i - h_{o,s}) \tag{6}$$

Similarly, outlet enthalpy of a compressor can be calculated

$$h_0 = h_i + \frac{(h_i - h_{o,s})}{y_s} \tag{7}$$

$h_0$ is the specific enthalpy at the outlet, $h_i$ being specific enthalpy at inlet, isentropic efficiency given by $\eta_s$ and when gas is isentropically expanded, specific enthalpy hs. When enthalpies change and level of turbine power is known, the mass flow necessary may be calculated.

## 2. Calculations of both systems

### 2.1. Initial assumptions

The base case system as given in Fig. 1 follows assumptions and input parameters. The modelling of gasifier is done as discussed above in gasifier subsystem. The solid carbon remaining, and tar formation is separated out by a separator. Tar formation was not taken into account for thermodynamic calculations. The biomass composition considered for the gasifier feed in mentioned in Table 1. To tabulate the trend in change of system efficiencies both Fig. 1 and Fig. 2 schemes have undergone increase in carbon dioxide percentage which will be further drawn out in the results section of this paper.(See Figs. 3-8).

### 2.2. Base case & enhanced carbon dioxide systems

At temperatures close to exit of gasifier at 977 K, a portion of gas cleaning may be done. The recommended gas- cleaning system contains a ceramic particulate filter that operates at 977 K. Tar is subsequently cleaned in a dolomite- based reactor. Particulate and tar-cleaning devices are shown by apparatus no. 103,703 in Fig. 1 and Fig. 2 respectively. At this stage, an alkali getter can also be advised. Gas temperatures are lowered for HCl, $H_2S$ and $SiO_2$ cleaning after particle and tar cleaning is completed. A system of two heat exchangers is used to cool biosyngas from 945 K to 873 K in base case system and 977 K to 873 K in enhanced carbon dioxide scheme. Since preheated steam helps in reduction of carbon deposition at zones with lower temperature where gas travels through before accessing the fuel cell the gas passes through before entering the fuel cell, it is injected before the temperature of the gas is lowered. After that, the gas is cooled down to 873 K to remove the HCl and $H_2S$.A sodium carbonate-based reactor cleans HCl, while a zinc titanate-based reactor cleans $H_2S$. Both HCl and $H_2S$ cleaning apparatus no. 107,707 are represented in Figs. 1 & 2 respectively. The initial heat exchanger decreases the temperature to 945 K, and the second heat exchanger uses an extra supply of air to lower the temperature to 905 K in the base case system shown here. Meanwhile, in the enhanced carbon dioxide scheme, the initial heat exchanger drops the temperature to 945 K, and the second heat exchanger uses an extra supply of air to lower the temperature to 873 K. The compressed air for the cathode is heated with this heat exchanger providing hot air. Following the HCl, $SiO_2$ and $H_2S$ cleaning, the heated gas using the first heat exchanger forms a mixture with a percentage of the anode outlet to raise the gas temperature to the fuel cell inlet temperature of 1073 K. At this phase, the higher hydrocarbons in the gas are catalytically cracked using a nickel-based tar cracker. A second alkali getter is used to reduce alkalis emitted by the HCl cleaning section. Final particle, tar, and alkali cleaning equipment are represented by apparatus no. 109 in Fig. 1 and apparatus no.708 in Fig. 2.

Gas-cleaning devices are thought to produce pressure dips. The aggregate pressure loss in the cleaning equipment sums to 0.12 bar for both schemes. The loss of heat to the environment from the entire system is believed to be insignificant. Clean gas is supplied to SOFC in both setups described here. Since the fuel gas is likely to contain a few ppm of $H_2S$, an extra internal sulfur-tolerant methane reformer with direct heat exchange with the stack and

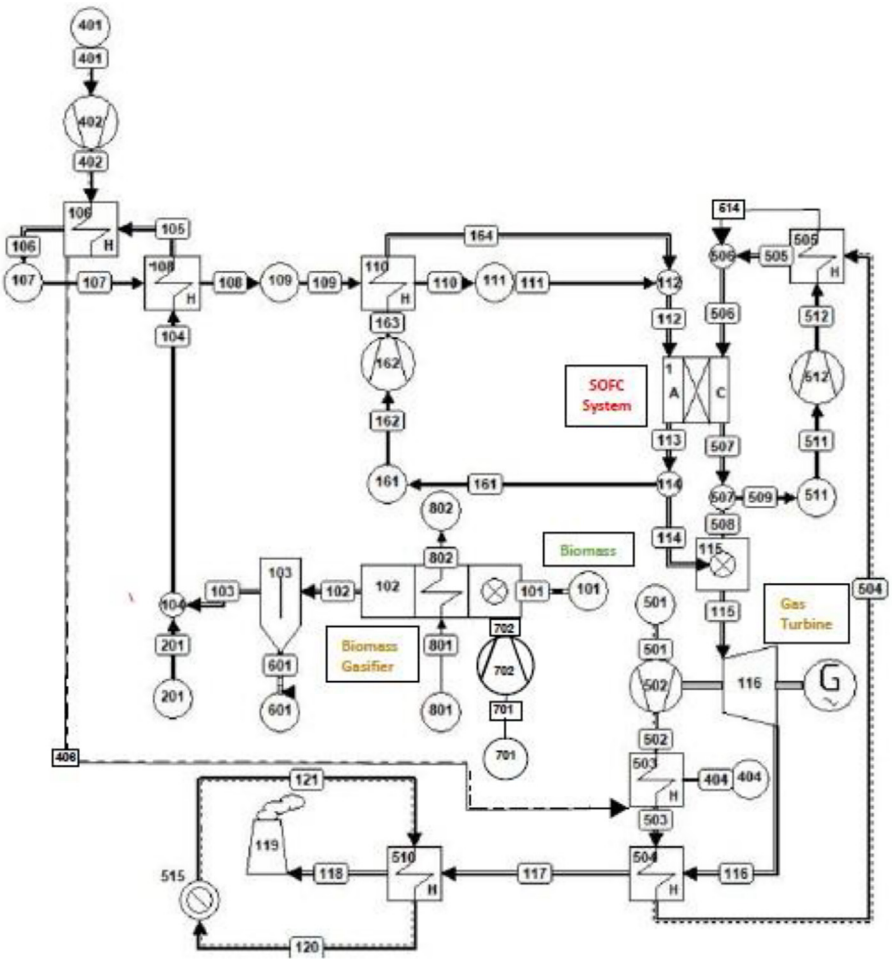


**Fig. 1.** Scheme for the Base Case System.

**Table 1**
Composition of Biomass.

| Components | Mass% |
|---|---|
| C | 39.41 |
| CH 4 | 4.08 |
| H H2O N O2 | 4.19 |
| S | 15.00 |
| SiO2 | 0.47 |
| | 36.12 |
| | 0.05 |
| | 0.68 |

operation at stack temperature is envisaged. A portion of the gas is recirculated, and the rest is delivered to the combustor exit, which is at 1273 K. The fuel gas temperature is raised to 1173 K after mixing with the anode exit gas which was recirculated. Air for the fuel cell is pressurized in compressor 502(both systems), which in fact is part of the gas-turbine-system, with turbine 116,717 driving both compressor and the electric generator and combustor apparatus no.115,716 of both systems respectively.

The cathode air is compressed before being heated, utilizing the heat wasted from the fuel gas purification system. Since mass moves along the system, the turbine power, which is fixed at 30 kW, determines the power level. The outlet gas from turbine is utilized to preheat the cathode air, gasification air, and the added steam. The process plan includes a sink that represents a heat consumer, to recover thermal energy situated at exit which will recover heat, where the gas temperature is decreased to 343 K before the stack receives it. The system calculations for a 30-kW hydrocarbon-fueled capstone gas turbine system have been published [14]. Using turbine and compressor at 78% isentropic efficiencies, 98% mechanical efficiencies have demonstrated, a system efficiency of roughly 30% may be achieved. This is compatible with the manufacturer's estimated efficiency of 30%. As a result, those isentropic, mechanical efficiencies are also used in the current estimates. System calculations with a hydrocarbon fuel for a commercial Capstone gas turbine system of 30 kW power have been published in the literature [14]. As a result, those isentropic and mechanical efficiencies are also included in the current estimates.

In enhanced carbon dioxide system, the compressed air is preheated in heat exchanger no.503, using heat, recovered from the gas- cleansing-system. Next it is preheated in heat exchanger no.504, recovering heat from the gas turbine exhaust. Then the air is heated by mixing it with recirculated air from the fuel cell cathode exit stream. The same method is used like for the anode (fuel-side). In afterburner apparatus no. 716, the left-over-fuel is combusted, using the surplus-air from the cathode. The hot flow is expanded in the turbine. Heat from the hot flue-gas is recovered from turbine. Initially the air for the fuel cell is preheated. Next the air and the $CO_2$ for the gasifier is preheated and finally the remaining heat is recovered for heating purposes in heat exchanger 301. Heat sink apparatus no. 302 shows the amount of available heat.

Table 2 lists values for key parameters utilized in calculation. Studies using diverse gas compositions which include biosyngas

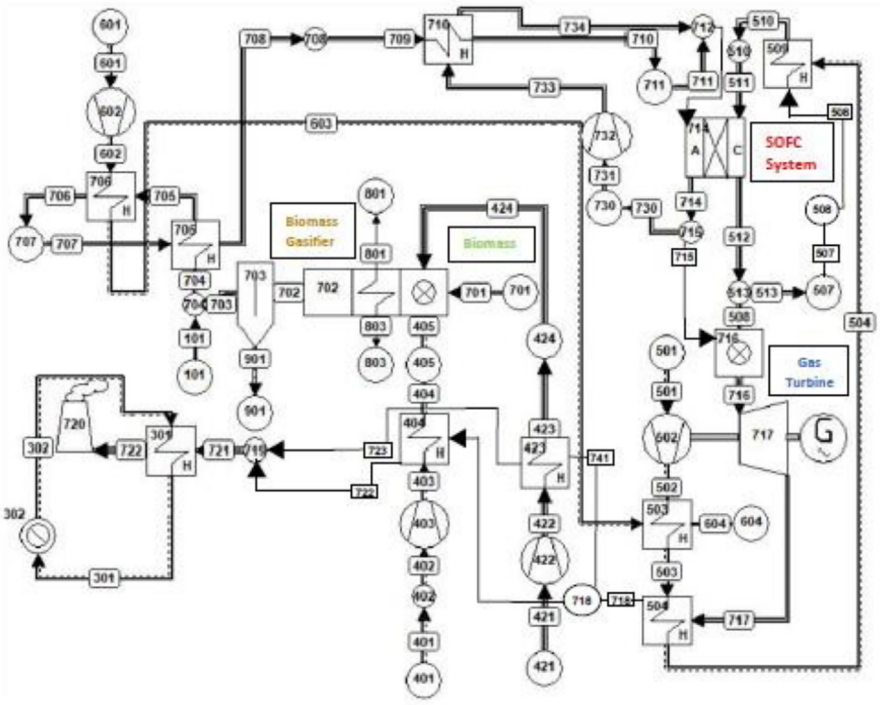


**Fig. 2.** Scheme for the Enhanced Carbon Dioxide System.

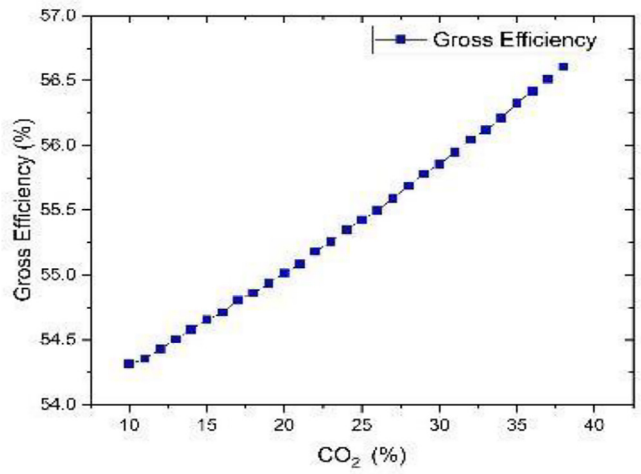


**Fig. 3.** Carbon Dioxide Vs Gross Efficiency in Carbon Dioxide Enhanced scheme.

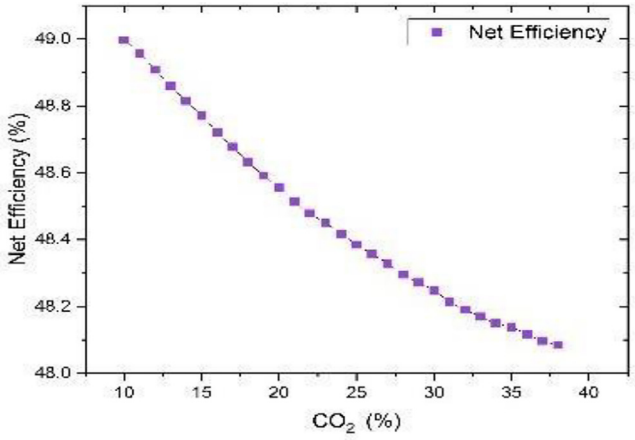


**Fig. 4.** Carbon Dioxide Vs Net Efficiency in Carbon Dioxide Enhanced scheme.

had been conducted on Ni/GDC anodes [1,5]. Acceptable values based on these findings for different SOFC model input parameters were assumed for the current calculations. At 1123 K, cell resistance is $6 \times 10^{-5}$ohm $m^2$ and at 1193 K, it is $3 \times 10^{-5}$ohm $m^2$. Cell resistance is assumed to be $5 \times 10^{-5}$ohm $m^2$ at an average SOFC temperature of 1223 K in the current calculations as a reasonable approximation. The average current density is 2500 A $m^{-2}$.

The percentage of fuel used is assumed to be 85 percent. The mean of inlet and outlet values (Before mixing with the recirculated anode outlet gas 85% of the incoming fuel) is used to calculate cell temperature and pressure data.

The process plan includes a sink that represents a heat consumer recover thermal energy a stack at the exit, where the temperature of gas is decreased to 343 K before being delivered it to the stack. A pressure drop of 0.05 bar across the fuel cell is considered. The pressure drop in the combustor is 0.02 bar. The software calculates the cell resistance itself. Current-density and the resistance of the fuel-cell cannot be assigned. The voltage and the current density must be assigned, and resistance will be calculated. The optimal voltage was found to be 0.7628 V and 0.7177 V for both schemes respectively.

## 3. Results & discussion

When Nernst voltage is proportional to pressure, as given by Eq. (2), SOFC performance should improve as pressure rises [1]. However, at lower pressure ratios, recuperated gas turbines exhibit higher efficiencies [15]. The system calculations in this paper are for a gas turbine cycle with an inlet pressure of 6 bar. The pressure ratios reported are between the inlet and outlet pressures (absolute pressure values) for gas turbine system compressor (Apparatus no. 502 in Figs. 1 & 2). The system efficiencies for the base

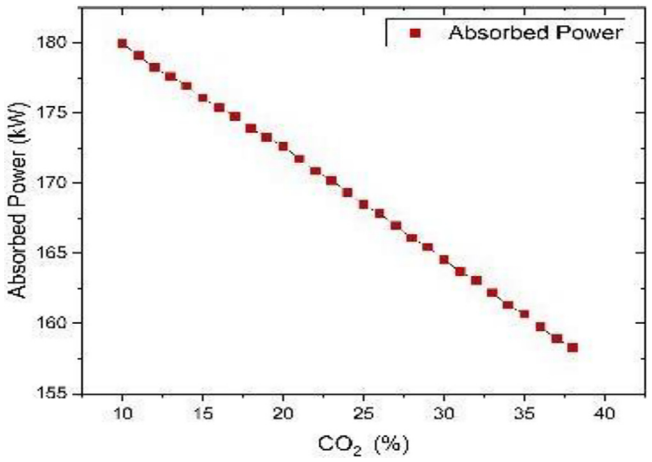


**Fig. 5.** Carbon Dioxide Vs Absorbed Power in Carbon Dioxide Enhanced scheme.

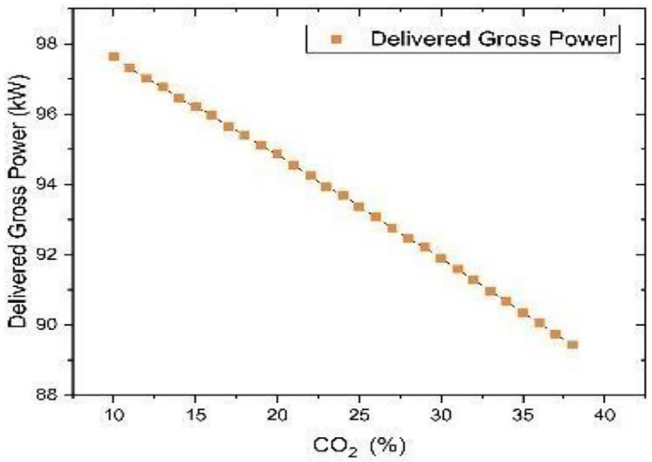


**Fig. 6.** Carbon Dioxide Vs Delivered Gross Power in Carbon Dioxide Enhanced scheme.

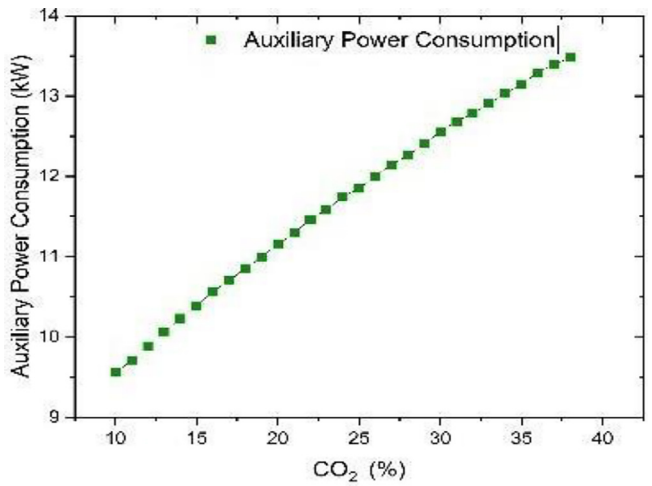


**Fig. 7.** Carbon Dioxide Vs Auxiliary Power Consumption in Carbon Dioxide Enhanced scheme.

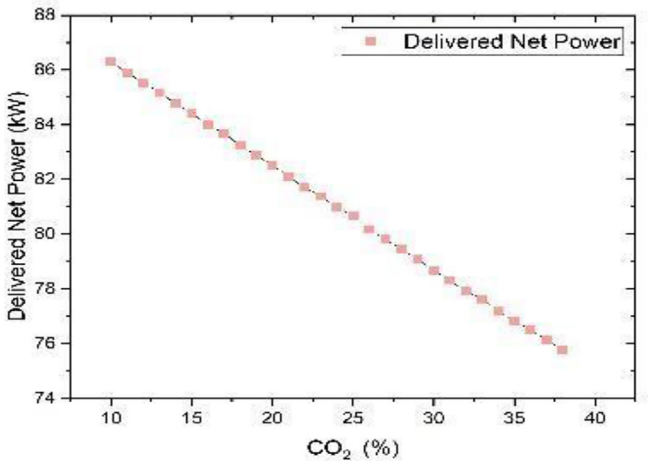


**Fig. 8.** Carbon Dioxide Vs Delivered Net Power in Carbon Dioxide Enhanced scheme.

**Table 2**
Input parameters of Both Schemes.

| Input parameters for various system components | |
|---|---|
| Isentropic efficiency for gas turbine (116) (717) | 78% |
| Isentropic efficiency for gas turbine compressor (502) | 78% |
| Mechanical efficiency for gas turbine (116) (717) | 98% |
| Mechanical efficiency for gas turbine compressor (502) | 98% |
| Isentropic efficiencies for other compressors and pumps | 75% |
| Mechanical efficiencies for other compressors and pumps | 95% |
| Generator | 90% |
| DC/AC conversion efficiency | 97% |
| Cell resistance | 5x $10^{-5}$ O $m^2$ |
| Current density | 2500 $Am^{-2}$ |
| Fuel utilization | 85% |

**Table 3**
System efficiency of Base case Scheme.

| | Apparatus | Energy [kW]Totals[kW] |
|---|---|---|
| Absorbed Power | Sink/Source | 173.74173.74 |
| Delivered Gross Power | Generator | 30 |
| | Fuel Cell | 69.3599.35 |
| Auxiliary Power Consumption | | 6.48 |
| Delivered Net Power | | 92.87 |
| Delivered Heat | Heat Sink | 69.0269.02 |
| Total Delivered | | 161.89 |
| Efficiencies | | |
| Gross | | 57.182 |
| Net | | 53.453 |
| Heat | | 39.724 |
| Total | | 93.177 |

**Table 4**
System efficiency of Enhanced Carbon Dioxide Scheme.

| | Apparatus | Energy [kW]Totals[kW] |
|---|---|---|
| Absorbed Power | Sink/Source | 157.48157.48 |
| Delivered Gross Power | Generator | 30 |
| | Fuel Cell | 59.2389.23 |
| Auxiliary Power Consumption | | 7.80 |
| Delivered Net Power | | 81.43 |
| Delivered Heat | Heat Sink | 66.0766.07 |
| Total Delivered | | 147.50 |
| Efficiencies | | |
| Gross | | 56.660 |
| Net | | 51.709 |
| Heat | | 41.953 |
| Total | | 93.661 |

case scheme and the improved carbon dioxide systems from cycle tempo are shown in Tables 3 and 4 respectively.

The carbon dioxide content in natural air composition was increased in enhanced carbon dioxide system by changing the $CO_2$ to fuel ratio where 10% mol of $O_2$ mixes with the carbon dioxide stream. This continued until the gasifier outlet temperature became too low or the fuel cell temperature became too high, resulting in a $CO_2$ and $O_2$ shortage. Every time composition is changed by increasing carbon dioxide content, variants of the discussed schemes are created, and the readings of variants are recorded. Here we will discuss the trends in system efficiency for enhanced carbon dioxide system when carbon dioxide content is enhanced.

Gross Efficiency is the ratio of electricity produced to heat absorbed by the system.

When auxiliary power is deducted from electricity produced it is termed as Net efficiency.

Absorbed Power is the heat send to the system, in general this will be the product of heating value and mass flow of fuel.

Delivered Gross Power is the mechanical or electrical power, delivered by the system, but excluding the auxiliary power-consumption.

Auxiliary power consumption is the power required for pumps and so on, as far as they are electrically driven.

Delivered Net Power is the net power of the system, being the (gross power minus the auxiliary power). In general, this will be the power that is sent to the grid.

## 4. Conclusion

Upon evaluating trends in system efficiency when $CO_2$ % was increased, delivered gross power kept decreasing for enhanced $CO_2$ % scheme. This is because the turbine power rating fixed at 30 kW, the energy flow in the fuel cell kept decreasing for each variant of enhanced system. Auxiliary power consumption was increasing in enhanced scheme as carbon dioxide to fuel ratio was increased. This is because compressors in enhanced scheme consume more power. The behavior of delivered net power graphs depends on delivered gross power & auxiliary power consumption relations depicting the decreasing trend in the enhanced scheme when $CO_2$ to fuel ratio increased. Absorbed power which deals with flow of energy in sources / sinks was lower in enhanced scheme. Delivered heat by heat sink was lower in enhanced scheme. Increased auxiliary power consumption in enhanced scheme followed a downward decreasing trend for net efficiency. The system has a steadily increasing trend for gross efficiency. Enhanced carbon dioxide scheme system seems to have a slightly higher total electrical efficiency by a close range of less than 1%. Further research must be done to interpret the decline in power generation.

## Data availability

Data will be made available on request.

## Declaration of Competing Interest

The authors declare that they have no known competing financial interests or personal relationships that could have appeared to influence the work reported in this paper.

## References

[1] P.V. Aravind, Studies on high efficiency energy systems based on biomass gasifiers and solid oxide fuel cells with Ni/GDC anodes, PhD Thesis, 2007, TU Delft
[2] P.V. Aravind, J.P. Ouweltjes, E. de Heer, N. Woudstra, G. Rietveld, Electrochem. Soc. Proc. 7 (2005) 1459–1467.
[3] P.V. Aravind, J.P. Ouweltjes, N. Woudstra, G. Rietveld, Electrochem. Solid State Lett. 11 (2008) B24–B28.
[4] S. Baron, N. Brandon, A. Atkinson, B. Steele, R. Rudkin, J. Power Sources 126 (2004) 58–66.
[5] J.P. Ouweltjes, P.V. Aravind, N. Woudstra, G. Rietveld, J. Fuel Cell Sci. Technol. 3 (2006) 495–498.
[6] K.D. Panopoulos, L.E. Fryda, J. Karl, S. Poulou, E. Kakaras, Journal of Power Sources 159 (1) (2006) 570– 585 C.
[7] Athanasiou, F. Coutelieris, E. Vakouftsi, V. Skoulou, E. Antonakou, G. Marnellos, A. Zabaniotou, International Journal of Hydrogen Energy 32 (3) (2007) 337–342
[8] A.O. Omosun, A. Bauen, N.P. Brandon, C.S. Adjiman, D. Hart, J. Power Sources 131 (1–2) (2004) 96–106.
[9] P.V. Aravind, MSc Thesis, University of Oldenburg, 2001.
[10] C. Bang-Møller, M. Rokni, B. Elmegaard, J. Ahrenfeldt, U.B. Henriksen, Decentralized combined heat and power production by two-stage biomass gasification and solid oxide fuel cells, Energy 58 (2013) 527–537.
[11] A. Baldinelli, L. Barelli, G. Bidini, Performance characterization and modelling of syngas-fed SOFCs (solid oxide fuel cells) varying fuel composition, Energy 90 (2015) 2070–2084.
[12] E. Shayan, V. Zare, I. Mirzaee, On the use of different gasification agents in a biomass fueled SOFC by integrated gasifier: a comparative exergo-economic evaluation and optimization, Energy 171 (2019) 1126–1138.
[13] R.Ø. Gadsbøll, J. Thomsen, C. Bang-Møller, J. Ahrenfeldt, U.B. Henriksen, Solid oxide fuel cells powered by biomass gasification for high efficiency power generation, Energy 131 (2017) 198–206.
[14] B.J.P. Burhe, MSc Thesis, Technical University Delft, 2000.
[15] H. Cohen, G. Rogers, H. Saravanamuttoo, Gas Turbine Theory, Addison Wesley Longman Limited, 1996.
[16] www.cycle-tempo.nl.